Full Paper

Propellants, Explosives, Pyrotechnics

DOI: 10.1002/prep.202000313

Simulation of Heat Flow Curves of NC-Based Propellants – Part 2: Application to DPA Stabilized Propellants

Daniel G. Itkis[a] and Manfred A. Bohn*[a]

Dedicated to Dr. Norbert Eisenreich (1948–2019), scientist at Fraunhofer ICT

Abstract: Measuring of heat flow curves at temperatures near the in-service range have become a standard for stability and compatibility assessments of nitrocellulose (NC)-based energetic materials. The typical technique to realise this demand is heat flow microcalorimetry. The heat flow curves are the summarized effect of the rates of all the reaction heats in the mixture. The propellant composition has a significant influence on the shapes of the heat flow curves. To assess the stability on a firmer base, it is of interest to know what contributions to the total heat flow the individual reactions have from the NC decomposition and from the stabilizer reactions. This needs the simulation of the heat flow curves based on the individual reactions with their thermochemical data and their reaction rates. For this, the reaction enthalpies of all relevant reactions must be known. On these prerequisites was reported in part 1. With the data from there, the simulation of the heat flow curve of the ball powder propellant type K6210 was undertaken, using a reaction scheme for the nitrate ester decomposition and the DPA reactions. In principle, the here developed and applied procedure is usable for all types of NC-based propellants and heat flow curves.

Keywords: simulation of heat flow curves · NC propellants · reaction schemes · reaction rate schemes · reaction enthalpies

1 Introduction

For NC-based materials (single to triple base gun propellants and double base rocket propellants) the determination of the isothermal heat flow with microcalorimeters is an established method now. The measured heat flow is a summation of all heat flow effects produced from all reactions going on in the material, meaning all exothermal and endothermal effects are summed up. For assessment of stabilizers, it is of interest to assign the parts of this gross heat flow to the individual reactions of NC and the stabilizer reactants.

For achieving the aim to simulate heat flow curves the necessary decomposition reactions of NC and the stabilizer reactions must be known, with their enthalpies of reaction. In part 1 of this publication unit [1] on 'Simulation of Heat Flow Curves of Propellants' the decomposition reactions of nitrocellulose (NC) and nitroglycerine (NG) were considered as well as the reactions of stabilizer diphenylamine (DPA). With the resulting data on the reaction enthalpies, the here intended task could be performed together with the application of a reaction scheme consisting of the number of necessary reactions. In principle, the presented procedure can be applied directly to other DPA stabilized propellants. Also, propellants with other stabilizers can be analysed by this method.

2 Simulation of Isothermal Heat Flow Curves

The isothermal heat flow curves also called heat generation rate curves, show propellant type-dependent appearance. Similarities occur with the same stabilizer and similar composition.

In Figure 1 four examples of heat flow curves are shown for typical gun propellants, measured at 80 °C in well-filled closed glass ampoules with residual air. Basic compositions of these propellants can be found in Table 1. Two propellants with Ak II stabilization show similarities. The single-base propellant of A5020 type has the lowest heat generation rates over the measured period. Pronounced features are shown by the spherical or ball powder (BP) propellant K6210, a double base propellant stabilized by DPA. These special features in the heat flow curve gave much attraction to this propellant. It was intensively and extensively investigated in the 1990 and the beginning of the first dec-

[a] *D. G. Itkis, M. A. Bohn*
Fraunhofer-Institut für Chemische Technologie (ICT)
Joseph-von-Fraunhofer-Straße 7, 76327 Pfinztal, Germany
**e-mail: Manfred.Bohn@ict.fraunhofer.de*

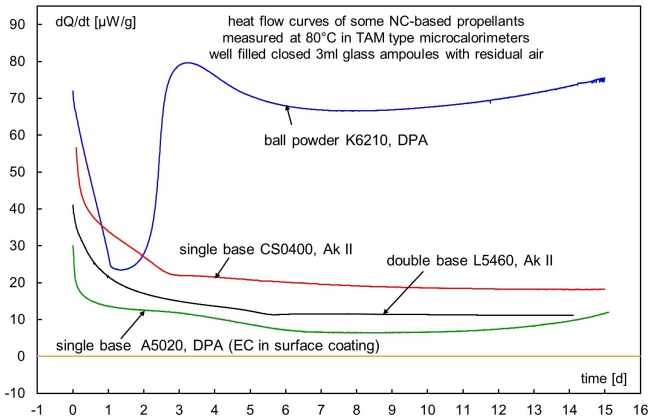

Figure 1. Isothermal heat flow curves dQ/dt of four NC-based propellants with their stabilizers. All measurements were performed at 80 °C in 3 ml well-filled glass ampoules with residual air, at Fraunhofer ICT with TAM™ generation II microcalorimeter from former Thermometric AB, Sweden.

Table 1. Basic compositions in mass-% of the GPs shown in Figure 1.

	L5460	A5020	CS0400	K6210
type	db	sb	sb	db
surface phlegmatized	no	yes	no	yes
phlegmatizer	none	DBP, EC, 4.5	none	DBP, 4.5
geometry	cylinder	cylinder	cylinder	spherical
web	7 holes	1 hole	1 hole	–
stabilizer	Ak II, 1	DPA, 1	Ak II, 2.1	DPA, 1
NC	59.0	93.0	97.0	74.0
nitroglycerine	14.5	none	none	18.4
diglycol dinitrate	24.7	none	none	none
others	0.8	1.5	0.9	2.1
N content of NC	13.2	13.1	13.2	13.1

Table 2. Smoothed concentration data in mass-% of the stabilizer reactants in DPA stabilized BP K6210, on a base of the data given in [4]. At two times, 5 and 9 days, the values were interpolated from the neighbouring values.

time d	time s	DPA m-%	NNO-DPA m-%	4-NO_2-DPA m-%	2-NO_2-DPA m-%
0	0	0.5000	0.5500	0.0330	0.0310
1	86400	0.3100	0.7400	0.0380	0.0380
2	172800	0.1600	0.8700	0.0450	0.0480
3	259200	0.0420	0.9700	0.0460	0.0560
4	345600	0.0190	1.0000	0.0370	0.0440
5	432000	0.0185	1.0000	0.0325	0.0330
6	518400	0.0180	1.0000	0.0280	0.0220
7	604800	0.0130	0.9600	0.0240	0.0140
8	691200	0.0040	0.9100	0.0150	0.0100
9	777600	0.0030	0.8350	0.0095	0.0065
10	864000	0.0020	0.7600	0.0040	0.0030

ade of 2000, which means a lot of data on its behaviour were collected. It was chosen for the aim to simulate its heat flow curve. Because of its stability limitations in comparison to the other types of propellants, it gave the impetus to develop the so-called heat-flow STANAG [2] at former BICT Heimerzheim, Germany, from 1997 to 2009 also called WIWEB ASt Heimerzheim, Germany. The outline and basics of this STANAG can be found in [3].

2.1 Data on Ball Powder (BP) K6210

Besides the heat flow curve also experimental data on the reaction behaviour during the consumption of the stabilizer are needed. Data on the stabilizer reactants could be found in [4], determined during ageing in daily time intervals at 80 °C. Further data and discussions on the behaviour of BP K6210 are reported in [5]. A close inspection revealed scattering in the data. Smoothing was applied, which has not changed the basic characteristics of the data. The concentration data in mass-% at 80 °C are given in Table 2 in daily steps and are shown graphically in Figure 2.

To apply the stabilizer data, it is necessary to convert their concentrations from mass-% to molar ones. For this the molar mass (M) data of the reactants given in Table 3 were used and in Table 4 the converted data are listed. The molar masses of NG and of NC (M of NC depends on nitrogen content) are also included in Table 3. The way of calculation of the NC data can be found in section 2 of [6]. The Figure 3 shows a synopsis of stabilizer concentration courses and the heat flow curve, all at temperature-time load at 80 °C. To improve the numerical stability of the algorithms in the calculations, the data of the reactants given in Table 2 have been interpolated between each daily step by 10 values, which results in 101 data points per reactant. The data of the heat flow curve were reduced to 101 data points in the considered time range 0 to 10 days.

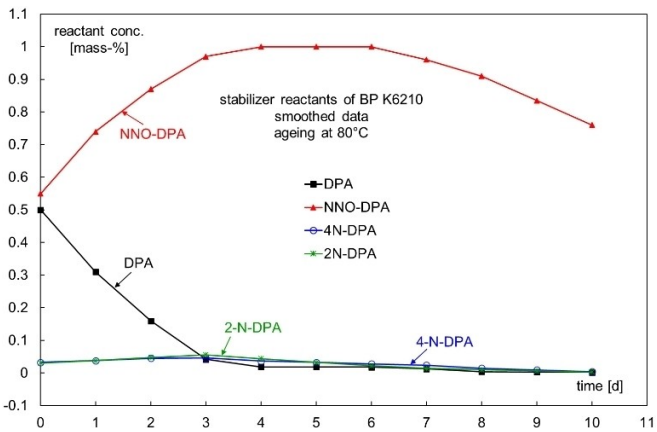

Figure 2. Concentration courses of the considered stabilizer reactants in BP K6210 aged at 80 °C.

Table 3. Molar masses M of the involved substances, including also higher nitrated DPA. With NC the molar mass M of half of the cellobiose unit (which has two AHG units) is given. The N-content of NC is in mass-%.

Substance	Molar mass M in g/mol
DPA	169.226
NNO-DPA	198.224
Mono-N-DPA	214.223
NNO-mono-N-DPA	243.221
Di-N-DPA	259.220
NG	227.085
NC (with N = 13.1 mass-%)	279.962

2.2 Reaction Scheme of the Stabilizer

Besides the decomposition reactions of NC and NG, reaction schemes for the stabilizer reactants must be considered. In a former work such reaction schemes have been developed already [7]. There also a DPA stabilized propellant was investigated. The reaction scheme RS III in [7] is taken and applied here. In this approach of the heat flow simulation method, the decomposition of NC and of nitroglycerine (NG) in producing the autocatalytically effective product P (see below) are considered together. This can be justified in that the concentration of NG is not to high, see Table 5, and one can assume a good gelatinization of NC with NG. This means the NG is 'confined' in the fibrillated superstructure of NC and not very mobile, and one can assume similar bond dissociation enthalpies in the CO-NO_2 bonds for both compounds, see [1].

The reaction equation system (RES) used here is given in Scheme 1. It contains nine reactions used to describe the reactant concentrations of the DPA series up to the first nitration step of DPA. NC stands here for the mixture of NC + NG. It contains the two decomposition channels of NC (NC + NG), and the reactions of DPA up to the mono-nitro-DPAs and including a back-reaction of NNO-DPA to DPA as well as the removal reactions of the three main products of DPA.

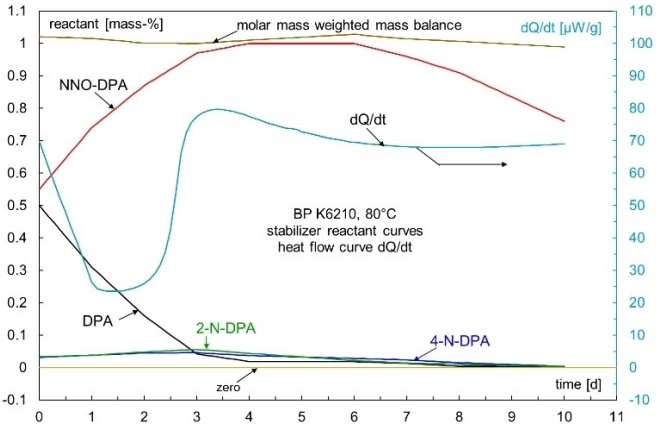

Figure 3. Synopsis of DPA reactant concentration courses and the heat flow curve dQ/dt of BP K6210 at 80 °C, the heat flow ordinate is on the right.

Table 5. Composition of ball powder K6210. With N = 13.1 mass-% the degree of substitution of the NC is 2.62.

	mass-%	
NC	74	
NC-N-content [mass-%]	–	13.1
Nitroglycerine (NG)	18.4	
DPA + NNO-DPA	0.9	
KNO_3	0.5	
Dibutyl phthalate	4.5	
Graphite	0.2	
volatile parts	1.5	
Sum	100	

The Scheme 2 shows the reaction rate equation system (RRES) corresponding to the RES of Scheme 1. It is a set of so-called ordinary differential equations of the first order, with given initial values for all variables. The task is to get the solution of Scheme 2, which means finally to get values for the reaction rate constants. This is achievable only nu-

Table 4. Smoothed concentration data in µmol/g of the stabilizer reactants in DPA stabilized BP K6210, on a base of the data given in Table 2. Recalculated from mass-% with the molar masses of the reactants.

time d	time s	DPA µmol/g	NNO-DPA µmol/g	4-NO_2-DPA µmol/g	2-NO_2-DPA µmol/g
0	0	29.5460	27.74600	1.54050	1.44709
1	86400	18.3187	37.33150	1.77385	1.77385
2	172800	9.45481	43.88974	2.10061	2.24066
3	259200	2.48189	48.93454	2.14730	2.61410
4	345600	1.12276	50.44798	1.72717	2.05393
5	432000	1.09321	50.44798	1.51711	1.54045
6	518400	1.06367	50.44798	1.30705	1.02697
7	604800	0.76820	48.43006	1.12033	0.65352
8	691200	0.23637	45.90766	0.70020	0.46680
9	777600	0.17728	42.12406	0.44346	0.30342
10	864000	0.11819	38.34046	0.18672	0.14004

$$
\begin{aligned}
&\mathrm{NC} \xrightarrow{k_{NC}} \mathrm{P} + \mathrm{R} && \Delta H_{R,NC}\\
&\mathrm{NC} + \mathrm{P} \xrightarrow{k_{auto}} 2\,\mathrm{P} + \mathrm{R} && \Delta H_{R,NC}\\
&\mathrm{DPA} + \mathrm{P} \xrightarrow{k_{NNO}} \mathrm{NNO\text{-}DPA} && \Delta H_{R,NNO}\\
&\mathrm{DPA} + \mathrm{P} \xrightarrow{k_{4N}} \mathrm{4N\text{-}DPA} && \Delta H_{R,4N}\\
&\mathrm{DPA} + \mathrm{P} \xrightarrow{k_{2N}} \mathrm{2N\text{-}DPA} && \Delta H_{R,2N}\\
&\mathrm{NNO\text{-}DPA} \xrightarrow{k_{DPNNO}} \mathrm{DPA} + \mathrm{P} && \Delta H_{R,DPNNO}\\
&\mathrm{NNO\text{-}DPA} + \mathrm{P} \xrightarrow{k_{NNO-}} \mathrm{DP_{NNO-}} && \Delta H_{R,NNO-}\\
&\mathrm{4N\text{-}DPA} + \mathrm{P} \xrightarrow{k_{4N-}} \mathrm{DP_{4N-}} && \Delta H_{R,4N-}\\
&\mathrm{2N\text{-}DPA} + \mathrm{P} \xrightarrow{k_{2N-}} \mathrm{DP_{2N-}} && \Delta H_{R,2N-}
\end{aligned}
\qquad (1)
$$

Scheme 1. Reaction equation system (RES) used in this study. P is the autocatalytic effective product. It may contain NO_2, HNO_2 and HNO_3. This reaction scheme is identical to RS III in [7].

$$
\begin{aligned}
\frac{dx_{NC}}{dt} &= -k_{NC}x_{NC} - k_{auto}x_{NC}x_P\\
\frac{dx_P}{dt} &= k_{NC}x_{NC} + k_{auto}x_{NC}x_P + k_{DPNNO}x_{NNO}\\
&\quad -(k_{NNO} + k_{4N} + k_{2N})x_P x_{DPA}\\
&\quad -(k_{NNO-}x_{NNO} + k_{4N-}x_{4N} + k_{2N-}x_{2N})x_P\\
\frac{dx_{DPA}}{dt} &= k_{DPNNO}x_{NNO} - (k_{NNO} + k_{4N} + k_{2N})x_P x_{DPA}\\
\frac{dx_{NNO}}{dt} &= k_{NNO}x_P x_{DPA} - k_{DPNNO}x_{NNO} - k_{NNO-}x_P x_{NNO}\\
\frac{dx_{4N}}{dt} &= k_{4N}x_P x_{DPA} - k_{4N-}x_P x_{4N}\\
\frac{dx_{2N}}{dt} &= k_{2N}x_P x_{DPA} - k_{2N-}x_P x_{2N}\\
\frac{dx_{NNO-}}{dt} &= +k_{NNO-}x_P x_{NNO}\\
\frac{dx_{4N-}}{dt} &= +k_{4N-}x_P x_{4N}\\
\frac{dx_{2N-}}{dt} &= +k_{2N-}x_P x_{2N}
\end{aligned}
\qquad (2)
$$

Scheme 2. Reaction rate equation system (RRES) corresponding to the RES of Scheme 1.

merically by 'integration' of the RRES using so-called Runge-Kutta (RK) procedures. In mathematical terms, it is a so-called 'initial value task' (initial value problem), which means to find the courses of the reactant concentrations starting from their initial values and using their coupled differential equations to establish the slopes to reach the next data points. Here the levels RK23 and RK45 have been used. There is no difference observable between these two RK levels because the curves are quite slowly changing in time. Both types adapt the step size. Level RK45 would be necessary for strong peak type functions. For the application, the tools and routines from OriginLab [8] have been used based on the program system OriginPro version 2019b.

The start values for the concentrations in the RRES are compiled in Table 6. For the autocatalytically effective reaction product P the start value of P(0) = 3 μmol/g was found by trying several start values. It was found that this value is best suited. It is reasonable because the measurement of heat flow at 80 °C produces already significant decomposition and the start value of P cannot be zero. P may consist of NO_2, HNO_2 and HNO_3, depending on the condition inside the propellant. Here we assume to have mainly NO_2. As discussed in Part 1 [1], till today the nature of P actually acting inside the NC and the propellant is still somewhat speculative, but the involvement of these three species is generally accepted. Further splitting of P in any number and types of species is not possible, as long as no quantitative determinations of them are achieved.

In Figures 4 to 6, the calculated concentrations in comparison to the experimental ones can be seen. The reproduction of the measured data is well. In Figure 4 the course of product P is shown and after the near consumption of primary stabilizer DPA its concentration raises. This shows the clearly less stabilizing activity of the consecutive products NNO-DPA and the two mono-nitro-DPAs. The Figure 5 shows with extended ordinate the concentration courses of the reactants with small concentrations. Figure 6 highlights the initial parts of the experimental and calculated concentration courses. In Table 7 the determined

Table 6. Start values (concentrations in μmol per g of propellant) of the quantities of the RRES for the numerical solution by RK methods. The start concentration of ONO_2 groups contains the ones of NC and NG together.

Start values and units		
t(0)	0	sec
total ONO_2(0)	9350.6	μmol/g
from NC ONO_2 (0)	6919.8	μmol/g
from NG ONO_2 (0)	2430.8	μmol/g
P(0)	3.0	μmol/g
DPA(0)	29.5460	μmol/g
NNO-DPA(0)	27.7460	μmol/g
4N-DPA(0)	1.54050	μmol/g
2N-DPA(0)	1.44709	μmol/g

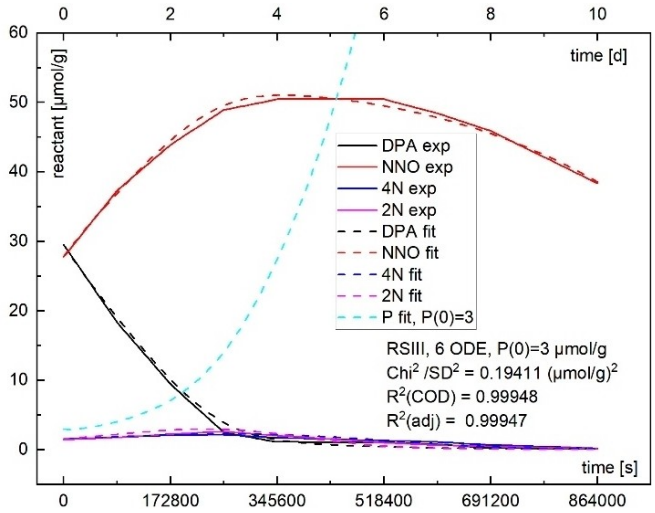

Figure 4. Comparison of calculated and experimental courses of the stabilizer reactants. Included is the time evolution of the autocatalytically effective product P, with P(0) = 3 µmol/g.

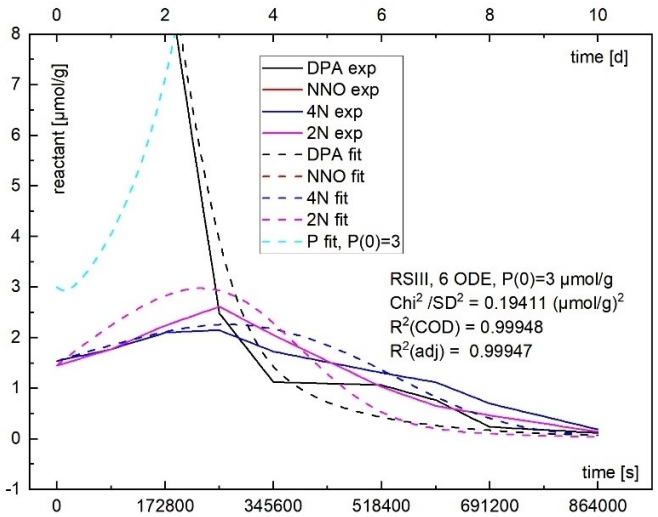

Figure 5. As Figure 4 before, with extended ordinate to show the reactants with small concentrations. NNO-DPA cannot be seen in this ordinate scale.

values for the nine reaction rate constants are listed, together with some parameters characterizing the fit quality.

3 Description of Heat Flow

3.1 Principle Formulation

In a substance, the total heat flow is the measured quantity $dQ_G(t)/dt$ at a given temperature. This total heat flow is comprised additively with heat flows of the individual reaction components K with their concentration change rates

Table 7. Result of the numerical integration of reaction rate equation system Eq. (2). The reaction rate constants were obtained by parameter variation in fitting Eq. (2) to the experimental data of Table 4, with extended data by interpolation up to 101 points for each reactant. The start value at P at time zero was set to 3 µmol/g.

property		value	std. dev.	units
k_{NC}	k1	1.307E-08	±2.53E-10	1/s
k_{auto}	k2	4.392E-10	±4.85E-11	g/µmol/s
k_{NNO}	k3	1.898E-06	±1.63E-07	g/µmol/s
k_{4N}	k4	5.104E-08	±6.34E-09	g/µmol/s
k_{2N}	k5	1.372E-07	±1.16E-08	g/µmol/s
k_{DPNNO}	k6	1.340E-06	±2.46E-07	1/s
k_{NNO-}	k7	3.246E-09	±6.35E-10	g/µmol/s
k_{4N-}	k8	7.485E-08	±1.04E-08	g/µmol/s
k_{2N-}	k9	2.585E-07	±2.55E-08	g/µmol/s
	P(0)	3.0	fixed	µmol/g
Fit quality				
	SD^2	0.19411		$(µmol/g)^2$
	FQS	76.6727		$(µmol/g)^2$
	R^2(COD)	0.99948		–
	R^2(adj)	0.99947		–
number of points		404		
degree of freedom		395		
parameter number		9		

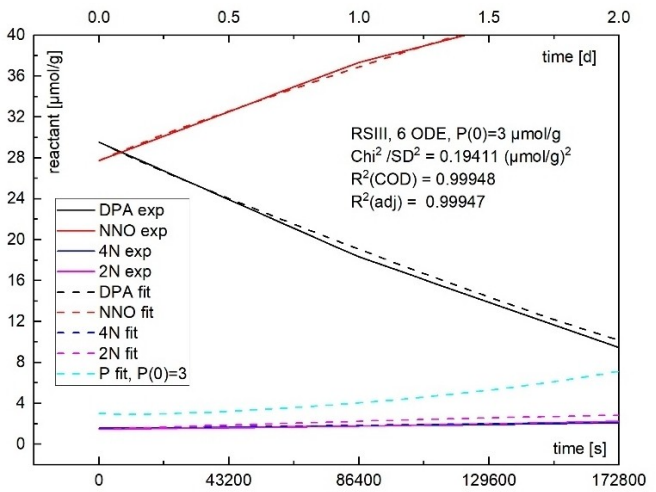

Figure 6. As Figure 4 before, with extended abscissa to show the evolution of DPA and NNO-DPA.

$dC_K(t)/dt$, which contribute each with the amount $dQ_K(t)/dt$, whereby the corresponding reaction enthalpy is the proportionality factor. This general formulation is given in Eq. (3). The often-used normalization by mass holds for each component with their respective mass part.

$$\frac{dQ_G(t)}{dt} = \sum_K \frac{dQ_K(t)}{dt} = -\sum_K \frac{dC_K(t)}{dt} \cdot (-\Delta H_{R,C_K}) \qquad (3)$$

$dQ_G(t)/dt$ total and measured heat flow
$dQ_K(t)/dt$ heat flow of the reaction of component K
$dC_K(t)/dt$ concentration change rate of component K
$(-\Delta H_{R,CK})$ reaction enthalpy of reaction of component K

The reaction enthalpy is a function of temperature. In heat flow measurements the exothermal effects are commonly taken with a positive sign, therefore the reaction enthalpy $\Delta H_{R,CK}$ is taken with a negative sign in Eq. (3). But the sign of the value of the reaction enthalpy entered into Eq.(3) follows the common rule (exothermal effects are counted negative). The following further sign rules apply to Eq. (3):

- Substances with decreasing concentrations have a negative sign;
- Substances with increasing concentrations have a positive sign;
- all $dQ_K(t)/dt$ will be added positively in the total equation.

3.2 Formulation of the Heat Flow Equation for BP K6210

Using the general expression of Eq. (3) to formulate the situation with the investigated propellant the following Eq. (4) to Eq. (7) result. Eq. (4) gives the full expression according to reaction scheme RES in Eq. (1) with the corresponding reaction enthalpies. The individual concentrations as a function of time have to be calculated with Eq. (2) after determining the reaction rate constants. It is also of interest how the individual reactions contribute to the measurable total heat flow. Three separate groups are considered with Eq. (5) to Eq. (7): (1) the part coming from the decomposition of the nitrate ester, (2) the part of the reactions of DPA and (3) the part of the removal reactions of the first stage DPA reaction products. One can separate Eq. (4) in all nine components, as will be shown in the next section. In Table 8 the naming convention is given and a set of values of the reaction enthalpies.

Table 8. Used namings of the quantities and the ranges of the estimated reaction enthalpies.

Used naming Concentrations of the reactants yj			Reaction rate constants kj		Reaction enthalpies Hj		Values of Hj kJ/mol	Ranges for Hj [kJ/mol]
x_{NC}	NC	y1	k_{NC}	k1	$\Delta H_{R,NC}$	H1	−80	−93.7 to −69.4 and to +161.5
x_P	P	y2	k_{auto}	k2	$\Delta H_{R,NC}$	H2	−80	−93.7 to −69.4 and to +161.5
x_{DPA}	DPA	y3	k_{NNO}	k3	$\Delta H_{R,NNO}$	H3	−87.3	until to −115
x_{NNO}	NNO-DPA	y4	k_{4N}	k4	$\Delta H_{R,4N}$	H4	−134.7	
x_{4N}	4N-DPA	y5	k_{2N}	k5	$\Delta H_{R,2N}$	H5	−124.9	
x_{2N}	2N-DPA	y6	k_{DPNNO}	k6	$\Delta H_{R,DPNNO}$	H6	87.3	until +115
x_{NNO-}	DP_{NNO-}	y7	k_{NNO-}	k7	$\Delta H_{R,NNO-}$	H7	−107.0	−90 to −130
x_{4N-}	DP_{4N-}	y8	k_{4N-}	k8	$\Delta H_{R,4N-}$	H8	−73.1	until to −135.4
x_{2N-}	DP_{2N-}	y9	k_{2N-}	k9	$\Delta H_{R,2N-}$	H9	−55.5	until to −135.4

$$\begin{aligned}\frac{dQ_G(t)}{dt} &= \\ &= \frac{dQ_{NC}(t)}{dt} + \frac{dQ_{auto}(t)}{dt} + \frac{dQ_{NNO}(t)}{dt} + \frac{dQ_{4N}(t)}{dt} + \frac{dQ_{2N}(t)}{dt} + \frac{dQ_{DPANO}(t)}{dt} + \frac{dQ_{NNO-}(t)}{dt} + \frac{dQ_{4N-}(t)}{dt} + \frac{dQ_{2N-}(t)}{dt} \\ &= +(-\Delta H_{R,NC})\cdot k_{NC}\cdot x_{NC}(t) \;+(-\Delta H_{R,NCauto})\cdot k_{auto}\cdot x_{NC}(t)\cdot x_P(t) \\ &\quad +(-\Delta H_{R,NNO})\cdot k_{NNO}\cdot x_{DPA}(t)\cdot x_P(t) \;+(-\Delta H_{R,4N})\cdot k_{4N}\cdot x_{DPA}(t)\cdot x_P(t) \;+(-\Delta H_{R,2N})\cdot k_{2N}\cdot x_{DPA}(t)\cdot x_P(t) \\ &\quad +(-\Delta H_{R,DPANO})\cdot k_{DPNNO}\cdot x_{NNO}(t) \\ &\quad +(-\Delta H_{R,NNO-})\cdot k_{NNO-}\cdot x_{NNO}(t)\cdot x_P(t) \;+(-\Delta H_{R,4N-})\cdot k_{4N-}\cdot x_{4N}(t)\cdot x_P(t) \;+(-\Delta H_{R,2N-})\cdot k_{2N-}\cdot x_{2N}(t)\cdot x_P(t)\end{aligned} \tag{4}$$

Part of the nitrate esters (NC, NG):

$$\begin{aligned}\frac{dQ_{NC}(t)}{dt} &= \frac{dQ_{NC}(t)}{dt} + \frac{dQ_{auto}(t)}{dt} \\ &= +(-\Delta H_{R,NC})\cdot k_{NC}\cdot x_{NC}(t) \;+(-\Delta H_{R,NCauto})\cdot k_{auto}\cdot x_{NC}(t)\cdot x_P(t)\end{aligned} \tag{5}$$

Part of the DPA reactions:

$$\frac{dQ_{DPA}(t)}{dt} = \frac{dQ_{NNO}(t)}{dt} + \frac{dQ_{4N}(t)}{dt} + \frac{dQ_{2N}(t)}{dt} + \frac{dQ_{DPANO}(t)}{dt}$$
$$= +(-\Delta H_{R,NNO}) \cdot k_{NNO} \cdot x_{DPA}(t) \cdot x_P(t) + (-\Delta H_{R,4N}) \cdot k_{4N} \cdot x_{DPA}(t) \cdot x_P(t)$$
$$+ (-\Delta H_{R,2N}) \cdot k_{2N} \cdot x_{DPA}(t) \cdot x_P(t) + (-\Delta H_{R,DPANO}) \cdot k_{DPNNO} \cdot x_{NNO}(t) \quad (6)$$

Part of the removal reactions of NNO, 4N, 2N:

$$\frac{dQ_{ABR}(t)}{dt} = \frac{dQ_{NNO-}(t)}{dt} + \frac{dQ_{4N-}(t)}{dt} + \frac{dQ_{2N-}(t)}{dt}$$
$$= +(-\Delta H_{R,NNO-}) \cdot k_{NNO-} \cdot x_{NNO}(t) \cdot x_P(t) + (-\Delta H_{R,4N-}) \cdot k_{4N-} \cdot x_{4N}(t) \cdot x_P(t)$$
$$+ (-\Delta H_{R,2N-}) \cdot k_{2N-} \cdot x_{2N}(t) \cdot x_P(t) \quad (7)$$

3.3 Result of Heat Flow Calculation with Set Parameters

With given values of the reaction rate constants kj and reaction enthalpies Hj the numerical integration of Eq. (4) can be done using the start values of the yj in Table 6 and using the start values for Q and dQ_G/dt here as 0 J/g and 69.7789 µW/g, respectively. Integration of Eq. (4) delivers the heat flow (heat generation) Q. In Figure 7 the result of the calculation of Q and dQ_G/dt is shown, using the data for the kj and Hj as given in Table 9. The qualitative congruence is acceptable. The values of the reaction rate constants are a bit changed against the data given in Table 7, but only in k3, k4 and k5. Also, the reaction enthalpy values are somewhat adapted. The result shows that probably not all essential reactions determining the heat flow are considered or that the reaction enthalpies are not yet the right ones.

The concentration courses of DPA and its products of this first calculation on the heat flow curve are presented in Figure 8 in comparison with the measurements.

The separation of the total heat flow in three parts as given in Eqs. (5) to (7) can be seen in Figure 9. The separation in further individual components is given in Figure 10. NC part means here the reaction of the ONO_2 groups of nitrocellulose and nitroglycerine. The intrinsic part (first reaction in Scheme 1) of the decomposition of the ONO_2 groups stays nearly constant over time, as it should be. The term 'intrinsic' describes the decomposition of NC by 'itself', which means only by the influence of temperature. It may be called unimolecular decomposition, but here this is a broader term, because the intrinsic comprises also the 'secondary' decomposition reactions after split-off of NO_2. The

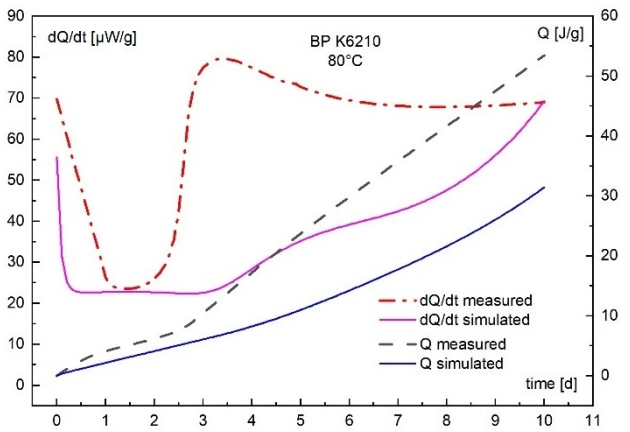

Figure 7. Result of the calculation of the heat flow curve dQ/dt and the heat Q of BP K6210. All reaction rate constants kj and reaction enthalpies Hj were set fixed, see Table 9, calculation here without parameter fitting. The qualitative congruence is already quite good.

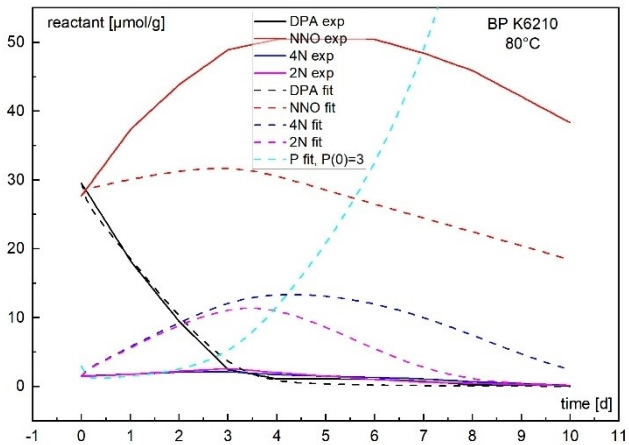

Figure 8. Comparison between the calculated curves (without parameter fitting) and the measured data of the stabilizer reactants.

Table 9. The used values for the nine reaction rate constants and the nine reaction enthalpies to calculate the total heat flow curve of BP K6210 given in Figure 7. No parameter fitting was applied; therefore, the standard deviations are zero. The dQ_G stands for dQ_G/dt.

		value	std. dev.	units
k_{NC}	k1	1.307E-08	0	1/s
k_{auto}	k2	4.392E-10	0	g/µmol/s
k_{NNO}	k3	2.000E-06	0	g/µmol/s
k_{4N}	k4	1.500E-06	0	g/µmol/s
k_{2N}	k5	1.500E-06	0	g/µmol/s
k_{DPNNO}	k6	1.340E-06	0	1/s
k_{NNO-}	k7	3.246E-09	0	g/µmol/s
k_{4N-}	k8	7.485E-08	0	g/µmol/s
k_{2N-}	k9	2.585E-07	0	g/µmol/s
	P(0)	3	fix	µmol/g
	Q(0)	0	fix	J/g
	$dQ_G(0)$	69.779		µW/g
$\Delta H_{R,NC}$	H1	−60	0	kJ/mol
$\Delta H_{R,NC}$	H2	−60	0	kJ/mol
$\Delta H_{R,NNO}$	H3	−90	0	kJ/mol
$\Delta H_{R,4N}$	H4	−134.7	0	kJ/mol
$\Delta H_{R,2N}$	H5	−124.9	0	kJ/mol
$\Delta H_{R,DPNNO}$	H6	90	0	kJ/mol
$\Delta H_{R,NNO-}$	H7	−106	0	kJ/mol
$\Delta H_{R,4N-}$	H8	−250	0	kJ/mol
$\Delta H_{R,2N-}$	H9	−250	0	kJ/mol

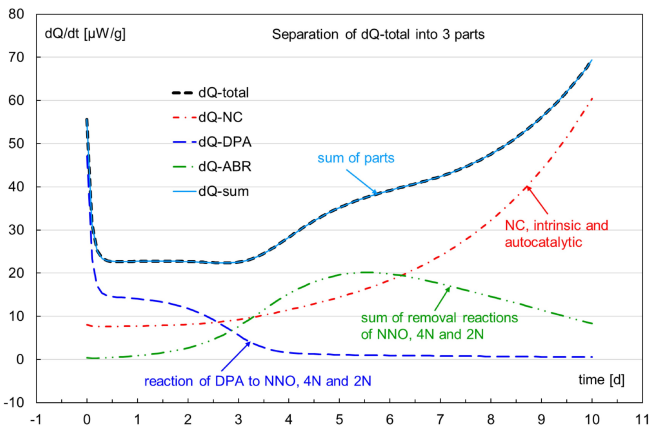

Figure 9. Separation of the simulated total heat flow in three parts: (1) NC part dQ-NC with the intrinsic and autocatalytic decomposition, (2) the reactions of DPA to NNO-DPA, 4N-DPA and 2N-DPA including the back reaction of NNO-DPA to DPA; (3) the sum of the removal reactions of NNO-DPA, 4N-DPA and 2N-DPA.

autocatalytic part (second reaction in Scheme 1) increases steadily, but at a higher rate when DPA is nearly consumed. The three consumption reactions of DPA provide nearly the same parts and the back reaction of NNO-DPA to DPA shows endothermal course with time, as it should be.

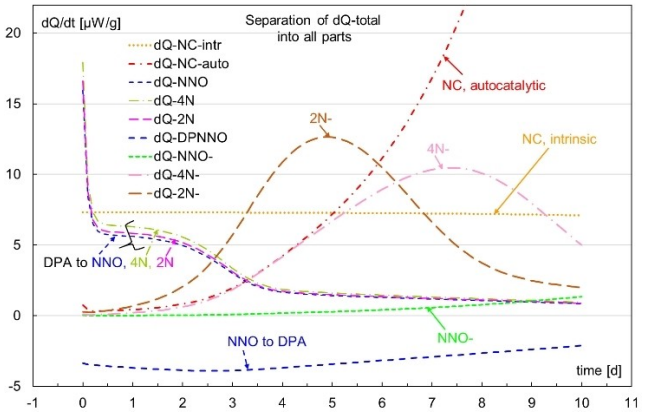

Figure 10. Separation of the simulated total heat flow in all nine single contributions according to the RES given in Scheme 1. The back reaction of NNO-DPA to DPA is endothermal. Here not to see is the total heat flow because of the ordinate scaling.

3.4 Result of Heat Flow Calculation with Controlled Parameter Fitting

A further calculation result is shown in Figure 11. The found parameters are compiled in Table 10. All parameters have been varied slowly and carefully to avoid the 'runaway' of the algorithm into unrealistic parameter values. The in total 18 fit parameters cannot be let in free variation. The calculated data Q and dQ/dt are in satisfying congruence with the measured data. The reproduction of the measured stabilizer reactants can be seen in Figure 12, also still in acceptable agreement.

Some of the reaction enthalpies are higher in value than estimated above. Especially the values of the removal reactions, H7, H8 and H9 are higher. This is interpreted as in-

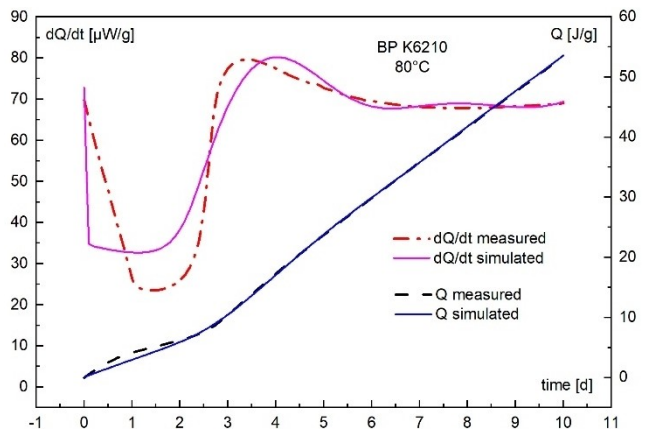

Figure 11. Result of the calculation using a parameter fitting in set limits of the values for kj and Hj. A satisfying description of the measured data is achieved. The values of kj and Hj are still in reasonable range, see Table 10.

Table 10. Result of the dQ/dt_Q calculation. The values of kj and Hj were varied all between set limits, in a step-by-step manner. The relative high values of H7, H8 and H9 indicate a sum of several reactions. The consecutive reactions are not yet separated in full.

		value	std. dev.	units
k_{NC}	k1	1.734E-08	3.50E-08	1/s
k_{auto}	k2	5.067E-10	2.90E-09	g/µmol/s
k_{NNO}	k3	1.500E-05	6.90E-05	g/µmol/s
k_{4N}	k4	2.504E-06	1.51E-04	g/µmol/s
k_{2N}	k5	1.911E-06	1.15E-04	g/µmol/s
k_{DPNNO}	k6	1.718E-06	6.80E-05	1/s
k_{NNO-}	k7	4.219E-08	4.40E-07	g/µmol/s
k_{4N-}	k8	3.984E-07	2.50E-05	g/µmol/s
k_{2N-}	k9	3.915E-07	3.10E-05	g/µmol/s
	P(0)	3	fix	µmol/g
	Q(0)	0	fix	J/g
	$dQ_G(0)$	69.779		µW/g
$\Delta H_{R,NC}$	H1	−254	193	kJ/mol
$\Delta H_{R,NC}$	H2	−13.4	231	kJ/mol
$\Delta H_{R,NNO}$	H3	−21.6	697	kJ/mol
$\Delta H_{R,4N}$	H4	−26.6	365	kJ/mol
$\Delta H_{R,2N}$	H5	−27.1	505	kJ/mol
$\Delta H_{R,DPNNO}$	H6	230	514	kJ/mol
$\Delta H_{R,NNO-}$	H7	−230	840	kJ/mol
$\Delta H_{R,4N-}$	H8	−629	700	kJ/mol
$\Delta H_{R,2N-}$	H9	−636	791	kJ/mol
Fit quality				
	SD^2	29.350		$(J/g)^2$
	FQS	5400.4		$(J/g)^2$
	R^2(COD)	0.958		–
	R^2(adj)	0.951		–
number of points		202		
degree of freedom		184		
parameter number		9 + 9		

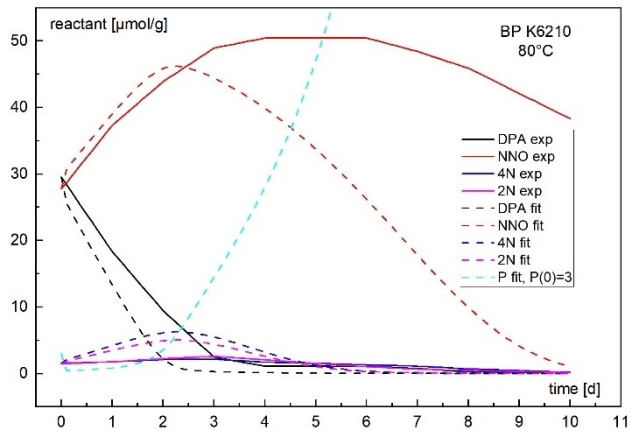

Figure 12. Comparison between the calculated curves and the measurements of the stabilizer reactants.

complete separation into the single reactions, therefore a summing up of reaction enthalpies occurs.

4 Summarizing Discussion

On the base of reactions in NC-based propellants stabilized with DPA and their reaction enthalpies determined with quantum mechanical methods (see part 1 of this publication unit [1]) the simulation of the heat flow curve of the double-base ball powder (BP) K6210 was tried. The experimental data available are the heat flow at 80 °C, measured in closed and well-filled 3 ml glass ampoules with a microcalorimeter (type TAM™) and the concentration courses of the DPA stabilizer series with time, obtained by HPLC on extracts from propellant samples aged also at 80 °C. At first, a reaction scheme has to be established, which includes the main NC reactions and the stabilizer reactions. For this, the so-called RS III was taken, developed already earlier to describe the stabilizer reactants in a DPA stabilized propellant [7]. With this reaction equations scheme consisting of nine reactions, the values of the nine corresponding reaction rate constants have been determined by numerical integration using tools from company OriginLab. The modelling of the stabilizer reactant concentration courses is with this reaction scheme very well. Together with the nine reaction rate constants obtained for BP K6210 and with the nine reaction enthalpies for these reactions at 80 °C, the first modelling of the heat flow curve was achieved without parameter fitting. The overall result is qualitatively already well. The separation of the total heat flow into the individual components was made and the obtained courses of the sub heat flows seem reasonable. The back reaction of NNO-DPA to DPA is endothermal and the heat flow of the intrinsic decomposition of NC stays constant as it should be. The three reactions of DPA to the three first consecutive products have a similar contribution, which is again reasonable taking into account the concentration courses and the reaction enthalpies. To handle 9 + 9 parameters is not an easy task. It was undertaken in the second modelling. The parameters were changed in a controlled way. A full free fit by the algorithm alone can be done, but the obtained parameter values are not realistic. Also with this controlled fitting, some reaction enthalpies can be interpreted as less real, especially the ones of the removal reactions of NNO-DPA, 4N-DPA and 2N-DPA. The deviations from the calculated reaction enthalpies are caused probably by missing reactions of consecutive stabilizer reactants. A free fit is with RS III (9 reactions and 9 fit parameters) and even the much larger system RS IV (22 reactions and 22 fit parameters), see [7], not such a problem because enough detailed data are available on the courses of the stabilizer reactants. With the reaction enthalpies, one has only one curve, the summarizing heat flow. With K6210 this curve is well structured in shape and information can be extracted via parameter fitting.

5 Conclusions

A simulation of the heat flow curve of the double-base ball powder propellant K6210, stabilized with DPA, was achieved using quantum mechanically based calculations of reaction enthalpies and the reaction rate constants obtained by modelling the experimental data of the reaction courses of the DPA-based reactants up to the mono-nitro-DPAs. In total nine reactions have been considered with nine reaction rate constants and nine reaction enthalpies. The simulation allows to look at the contributions of the individual reactions, this means a split of the total heat flow curves into individual heat flow curves. This possibility is of importance when assessing new stabilizers, to see the contributions of NC decomposition and the stabilizer reactions. This helps to get an evaluation of the effectiveness of a stabilizer. A low heat flow per se is not unique in the sense to have a good stabilizer because of the summed-up parts of all reactions going on. There might be endothermal reaction parts, which reduce the measurable total heat flow to low levels. But also, the reverse may happen, the stabilizer reactions could contribute to a higher level, but the decomposition rate of NC is nevertheless low. Despite the importance to fulfil a heat flow limit, one should have in mind that a stabilizer must be able to hold further quantities inside limit values. For example, stabilizer Ak II is seen as a good stabilizer in gun propellants, but it is inferior to 2-nitro-DPA in double base rocket propellants. With Ak II the gas generation inside the sample is higher than with 2-nitro-DPA, see [9].

With one simulation all $9+9$ parameters have been varied in a controlled manner. By this, a quantitatively acceptable simulation of the total heat flow was achieved. However, some reaction enthalpies are high in values, especially the ones of the removal reactions of NNO-DPA, 4N-DPA and 2N-DPA. This indicates a convolution of several reactions, which should be separated. Consideration of further stabilizer reactions beyond the first stage is necessary for this. Additional reactions of NC and NG should be considered also. First indications point to aldehydes to be included. With quantitative data on the stabilizer reactions, also propellants with other stabilizers can be analysed by this method, which is, therefore, a so-called generic one.

Symbols and Abbreviations

Names

BICT	Bundesinstitut für Chemisch-Technische Untersuchungen, 53913 Swisttal-Heimerzheim, Germany, up to 31 March 1997.
ICT	Fraunhofer-Institut für Chemische Technologie, 76318 Pfinztal-Berghausen, Germany.
Origin™	program system from company OriginLab Corporation, One Roundhouse Plaza, Suite 303, Northampton, MA 01060, USA.
WIWEB	Wehrwissenschaftliches Institut für Werk-, Explosiv- und Betriebsstoffe, 85435 Erding, Germany; from 1st April 1997, BICT was part of this institute as ‚WIWEB, Außenstelle Heimerzheim', up to 31 March 2009. Today part of the former BICT is included in WTD 91, 49716 Meppen, Germany. WIWEB changed name from 1st April 2009 on to WIWeB (now with lowercase e): Wehrwissenschaftliches Institut für Werk- und Betriebsstoffe.
WTD 91	Wehrtechnische Dienststelle für Waffen und Munition der Bundeswehr, D-49716 Meppen, Germany (Bundeswehr Technical Center for Weapons and Ammunition, WTD 91).
BAAINBw	Bundesamt für Ausrüstung, Informationstechnik und Nutzung der Bundeswehr, D-56073 Koblenz.

Chemical Terms

NC	nitrocellulose
NG	nitroglycerine, also Ngl
Ngl	nitroglycerine, also NG
P	stands for the autocatalytically effective products
AHG	anhydroglucose unit of NC
Ak II	Akardite II, stabilizer
EC	ethyl centralite, stabilizer
GP	gun propellant
BP	ball powder, means a spherical shape of the grains
sb	single base, propellants with only NC as energetic substance
db	double base, propellants with NC and NG (and /or other nitrate ester plasticizers) as energetic substances
K6210	spherical double base propellant
DPA	diphenylamine, stabilizer
NNO-DPA	N-nitroso-diphenylamine
NNO	same as NNO-DPA
4N-DPA	4-nitro-diphenylamine, 4-NO_2-DPA
4N	same as 4N-DPA
2N-DPA	2-nitro-diphenylamine, 2-NO_2-DPA
2N	same as 2N-DPA
NNO-	products of NNO removal reaction
4N-	products of 4N removal reaction
2N-	products of 2N removal reaction
$S_{E,Ar}$	electrophilic aromatic substitution
m.-%	mass-% (old term is weight-%)
µmol	concentration measure, micro-mol

TAM™	Thermal Activity Monitor, a type of microcalorimeter developed by Thermometric AB, 17561 Jarfälla, Sweden; now belonging to TA Instruments, Newcastle, Delaware, USA.
HFC	heat flow calorimeter heat flow calorimetry
HFMC	heat flow microcalorimeter
dQ/dt	isothermal heat flow, heat generation rate
dQ	same as dQ/dt
dQ_G/dt	total isothermal heat flow of sample
dQ_K/dt	isothermal heat flow of component K in sample
Q	heat evolved, heat generation
yj	individual reaction components, in short written
kj	individual reaction rate constants, in short written
Hj	individual reaction enthalpy, in short written
ΔH_R	reaction enthalpy
ΔH°_R	reaction enthalpy at standard condition
ΔG_R	reaction Gibbs free energy
ΔG°_R	reaction Gibbs free energy at standard condition
$\Delta_{bond}H$	bond dissociation enthalpy, also when formally calculated from dissociation reaction
$\Delta_{bond}G$	bond dissociation Gibbs free energy, also when formally calculated from dissociation reaction

Parameter fitting

ODE	ordinary differential equation
FitODE	tool from OriginLab to integrate a system of differential equations and simultaneously to fit the parameters to measured data of type integrated
RES	reaction equation system
RRES	reaction rate equation system
RS III	reaction scheme III, see [7]. The same as the RES given in Scheme 1
FQS	sum of squared deviation between model and measurement
n	number of points
p	number of fit parameters
SD^2	variance of fit, $SD^2 = FQS/(n-p)$
R^2(COD)	general correlation coefficient of fit (coefficient of determination)
R^2(adj)	adjusted correlation coefficient of fit $R^2(adj) = 1-(1-R^2(COD))*(n-1)/(n-p)$
RK23	Runge-Kutta (RK) integration level $2+3$; a combination of RK of order 2 and order 3 with implicit error control and step size control; Runge-Kutta procedures have been developed by the two German mathematicians Carl Runge and Martin Wilhelm Kutta; later Erwin Fehlberg (also German) provided further developments with respect to error control, see RK45.
RK45	Runge-Kutta integration level $4+5$, a combination of RK of order 4 and order 5 with implicit error control and step size control. The standard RK procedure is RK4.
RKF45	Runge-Kutta-Fehlberg integration of level $4+5$; same as RK45.

Acknowledgements

The authors thank Dr. Johannes Lang, Fraunhofer ICT, for hints on the use of quantum mechanical calculation techniques.

Dr. Michael Koch from WTD 91 (Bundeswehr Technical Center for Weapons and Ammunition, WTD 91), D-49716 Meppen, Germany is thanked for supporting this work and granting it via BAAINBw, Koblenz, Germany.

The company OriginLab is thanked for adapting and improving the tool FitODE and to provide special functions to perform the numerical integration of the differential equation system and the calculation of the heat flow curves. Special thanks to the German distributor of OriginLab, the company ADDITIVE Soft- und Hardware für Technik und Wissenschaft GmbH, D-61381 Friedrichsdorf, which always supported us in realizing our wishes.

This publication is based on the Bachelor thesis of Mr. Daniel G. Itkis in Chemistry at Ludwig-Maximilian-Universität, München, Germany.

Open access funding enabled and organized by Projekt DEAL agreement.

Data Availability Statement

The data that support the findings of this study are available in references given in the manuscript. They are available by the public.

References

[1] Daniel G. Itkis, Manfred A. Bohn. Simulation of Heat Flow Curves of NC-based Propellants – Part 1: Determination of reaction enthalpies and other characteristics of the reactions of NC and stabilizer DPA using quantum mechanical methods. *Propellants, Explosives, Pyrotechnics,* **2021**, 46. DOI: 10.1002/prep.202000314.

[2] NATO STANAG 4582 (Edition 1). Explosives, nitrocellulose-based propellants, stability test procedure and requirements using heat flow calorimetry. *NATO Headquarter Brussels; Allied Ordnance Publication* **2004**.

[3] Uldis Ticmanis, Stephan Wilker, Gabriele Pantel, Manfred Kaiser, Pierre Guillaume, Corinne Bales, Niels van der Meer. Principles of a STANAG for the estimation of the chemical stability of propellants by heat flow calorimetry. *Proceedings 31st International Annual Conference of ICT, pages 2–1 to 2–20.* June 27–30, 2000, Karlsruhe, Germany. Fraunhofer Institut für Chemische Technologie (ICT), D-76318 Pfinztal-Berghausen, Germany, **2000**.

[4] Pierre Guillaume, Mauricette Rat, Stephan Wilker, Gabriele Pantel. Microcalorimetry and chemical studies of double base propellants. *Proceedings of 29th International Annual Conference of ICT, pages 133–1 to 133–14.* June 30–July 3, 1998, Karlsruhe, Germany. Fraunhofer Institut für Chemische Technologie (ICT), D-76318 Pfinztal-Berghausen, Germany **1998**.

[5] Pierre Guillaume, Mauricette Rat, Gabriele Pantel Stephan Wilker, Heat Flow Calorimetry of Propellants – Effects of Sample Preparation and Measuring Conditions, *Propellants Explos. Pyrotech.* **2001**, *26*, 51–57.

[6] Manfred A. Bohn, Mohammed Moniruzzaman, John Bellerby. Modelling of the consumption of a dye used to probe the decomposition of nitrocellulose., *CD-Proceedings of the 45th International Annual Conference of ICT on 'Energetic Materials – Particles, Processing, Applications', pages 107–1 to 107–20.* June 24 to 27, 2014, Karlsruhe, Germany. ISSN 0722-4087. Fraunhofer-Institut fuer Chemische Technologie (ICT), D-76318 Pfinztal. Germany, **2014**. Paper available also by author MAB.

[7] Manfred A. Bohn, Norbert Eisenreich, Kinetic modelling of the stabilizer consumption and the consecutive products of the stabilizer in a gun propellant, *Propellants Explos. Pyrotech.* **1997**, *22*, 125–136. DOI: 10.1002/prep.19970220306.

[8] OriginLab Corporation, One Roundhouse Plaza, Suite 303, Northampton, MA 01060, USA. used program: Origin(Pro) Version 2019b, together with tool FitODE V1.3, as well as customer-specific tools.

[9] Manfred A. Bohn. Principles of ageing of double-base propellants and its assessment by several methods following propellant properties. *Presented at the NATO STO (Science & Technology Organization) Applied Vehicle Technology Panel (AVT) Collaboration Support Office, AVT-268 RSM-046 (Research Specialists' Meeting) on Advances in Munition Health Management Technologies and Implementation, paper MP-AVT-268-20.* October 9–11, **2017**, Utrecht, The Netherlands. Article available via MP-AVT-268-20.pdf or STO-MP-AVT-268 (nato.int).

Manuscript received: December 2, 2020
Revised manuscript received: February 28, 2021
Version of record online: May 26, 2021

